111, 3576; *Angew. Chem. Int. Ed.* **1999**, *38*, 3365; f) D. H. Camacho, I. Nakamura, S. Saito, Y. Yamamoto, *J. Org. Chem.* **2001**, *66*, 270.
[4] a) T. Mitsudo, Y. Hori, Y. Yamakawa, Y. Watanabe, *J. Org. Chem.* **1987**, *52*, 2230; b) D. M. T. Chan, T. B. Marder, D. Milstein, N. J, Taylor, *J. Am. Chem. Soc.* **1987**, *109*, 6385; c) B. M. Trost, W. Brieden, K. H. Baringhaus, *Angew. Chem.* **1992**, *104*, 1392; *Angew. Chem. Int. Ed. Engl.* **1992**, *31*, 1335; d) H. Doucet, B. Martin-Vaca, C. Bruneau, P. H. Dixneuf, *J. Org. Chem.* **1995**, *60*, 7247; e) M. Al-Masum, Y. Yamamoto, *J. Am. Chem. Soc.* **1998**, *120*, 3809.
[5] Review: a) T. Kondo, T. Mitsudo, *Chem. Rev.* **2000**, *100*, 3205; for hydrothiolation of alkynes, b) A. Ogawa, T. Ikeda, K. Kimura, T. Hirao, *J. Am. Chem. Soc.* **1999**, *121*, 5108.
[6] Addition of P–H bonds to alkynes: a) L.-B. Han, R. Hua, M. Tanaka, *Angew. Chem.* **1998**, *110*, 98; *Angew. Chem. Int. Ed.* **1998**, *37*, 94; b) M. A. Kazankova, I. V. Efimova, A. N. Kochetkov, V. V. Afanas′ev, I. P. Beletskaya, P. H. Dixneuf, *Synlett* **2001**, 497.
[7] Review: a) I. Beletskaya, A. Pelter, *Tetrahedron* **1997**, *53*, 4957; b) "Metal-catalyzed Hydroboration Reactions": G. C. Fu in *Transition Metals for Organic Synthesis* (Eds.: M. Beller, C. Bolm), Wiley-VCH, Weinheim, **1998**, pp. 141 – 146.
[8] Review: a) K. A. Horn, *Chem. Rev.* **1995**, *95*, 1317; b) "Hydrosilylation of Olefins": K. Yamamoto, T. Hayashi in *Transition Metals for Organic Synthesis* (Eds.: M. Beller, C. Bolm), Wiley-VCH, Weinheim, **1998**, pp. 120 – 129.
[9] Review: N. D. Smith, J. Mancuso, M. Lautens, *Chem. Rev.* **2000**, *100*, 3257.
[10] Diboration of alkynes: a) T. Ishiyama, N. Matsuda, N. Miyaura, A. Suzuki, *J. Am. Chem. Soc.* **1993**, *115*, 11018; b) T. Ishiyama, N. Matsuda, M. Murata, F. Ozawa, A. Suzuki, N. Miyaura, *Organometallics* **1996**, *15*, 713; c) G. Lesley, P. Nguyen, N. J. Taylor, T. B. Marder, A. J. Scott, W. Clegg, N. C. Norman, *Organometallics* **1996**, *15*, 5137; d) C. N. Iverson, M. R. Smith III, *Organometallics* **1996**, *15*, 5155.
[11] Review: M. Suginome, Y. Ito, *Chem. Rev.* **2000**, *100*, 3221.
[12] Silaboration of alkynes, a) M. Suginome, H. Nakamura, Y. Ito, *Chem. Commun.* **1996**, 2777; b) M. Suginome, T. Matsuda, H. Nakamura, Y. Ito, *Tetrahedron* **1999**, *55*, 8787.
[13] Disilylation of alkynes: a) H. Sakurai, Y. Kamiyama, Y. Nakadaira, *J. Am. Chem. Soc.* **1975**, *97*, 931; b) F. Ozawa, M. Sugawara, T. Hayashi, *Organometallics* **1994**, *13*, 3237.
[14] Silastannylation of alkynes: M. Hada, Y. Tanaka, M. Ito, M. Murakami, H. Amii, Y. Ito, H. Nakatsuji, *J. Am. Chem. Soc.* **1994**, *116*, 8754.
[15] E. Piers, R. T. Skerlj, *J. Chem. Soc. Chem. Commun.* **1986**, 626.
[16] a) H. Nakamura, M. Sekido, M. Ito, Y. Yamamoto, *J. Am. Chem. Soc.* **1998**, *120*, 6838; b) N. Moneiro, G. Balme, *Synlett* **1998**, 746; c) A. Fürstner, H. Szillat, F. Stelzer, *J. Am. Chem. Soc.* **2000**, *122*, 6785.
[17] Catalytic skeletal rearrangement: a) T. J. Katz, T. M. Sivavec, *J. Am. Chem. Soc.* **1985**, *107*, 737; b) A. Kinoshita, M. Mori, *Synlett* **1994**, 1020; c) B. M. Trost, G. J. Tanoury, *J. Am. Chem. Soc.* **1988**, *110*, 1636; d) B. M. Trost, M. K. Trost, *J. Am. Chem. Soc.* **1991**, *113*, 1850; e) B. M. Trost, A. S. K. Hashmi, *Angew. Chem.* **1993**, *105*, 1130; Angew. *Chem. Int. Ed.* **1993**, *32*, 1085; f) N. Chatani, T. Morimoto, T. Muto, S. Murai, *J. Am. Chem. Soc.* **1994**, *116*, 6049; g) N. Chatani, N. Furukawa, H. Sakurai, S. Murai, *Organometallics* **1996**, *15*, 901; h) N. Chatani, K. Kataoka, S. Murai, N. Furukawa, Y. Seki, *J. Am. Chem. Soc.* **1998**, *120*, 9104; i) ref. [16c].
[18] a) W. A. Herrmann, C.-P. Reisinger, M. Spiegler, *J. Organomet. Chem.* **1998**, *557*, 93; b) K. L. Greenman, D. S. Carter, D. L. Van Vranken, *Tetrahedron* **2001**, *57*, 5219; c) K. Miki, F. Nishino, K. Ohe, U. Sakae, *J. Am. Chem. Soc.* **2002**, *124*, 5260.
[19] B. H. Lipshutz, D. Pollart, J. Monforte, H. Kotsuki, *Tetrahedron Lett.* **1985**, *26*, 705.
[20] T. Soga, H. Takenoshita, M. Yamada, T. Mukaiyama, *Bull. Chem. Soc. Jpn.* **1990**, *63*, 3122.
[21] a) T. Kumamoto, N. Tabe, K. Yamaguchi, H. Yagishita, H. Iwasa, T. Ishikawa, *Tetrahedron* **2001**, *57*, 2717; b) V. M. Marathias, P. H. Bolton, *Biochemistry* **1999**, *38*, 4355; c) W. M. Clark, A. M. Ticker-Eldridge, G. Kris Huang, L. N. Pridgen, M. A. Olsen, R. J. Mills, I. Lantos, N. H. Baine, *J. Am. Chem. Soc.* **1998**, *120*, 4550.

Monodisperse Surface Micelles of Nonpolar Amphiphiles in Langmuir Monolayers**

Mounir Maaloum, Pierre Muller, and Marie Pierre Krafft*

There are several examples of surface micelles (hemimicelles) formed by self-assembly of small molecules and macromolecules that are adsorbed on solid surfaces and in equilibrium with aqueous solutions.[1] On the other hand, reports on surface micelles in Langmuir monolayers are essentially limited to copolymers.[2] Although their existence has long been predicted,[3,4] so far only one example of surface micelles made from small amphiphilic molecules exists.[5] These surface micelles were made from *strongly polar* surfactants. Furthermore no rule for predicting the size of the hemimicelles has been found. We report here on novel surface micelles made of a nonpolar amphiphile, namely, the semifluorinated alkane $C_8F_{17}C_{16}H_{33}$ (F8H16), their structure, and a model that accounts for their size.

Since the pioneering work of Gaines demonstrated that semifluorinated alkanes $C_nF_{n+1}C_mH_{2m+1}$ (F*n*H*m* diblocks) form Langmuir monolayers,[6] their structure has remained controversial. A primary issue was the orientation of the F*n*H*m* molecules at the air–water interface. Grazing-incidence X-ray diffraction (GIXD) and X-ray reflectivity (GIXR) studies on F12H18 concluded that the most probable arrangement was a monolayer in which the H*m* segments are in contact with water and the F*n* segments extend upwards from the surface.[7] However, a bilayer structure in which the diblocks are antiparallel, with tilted F8 segments outside and interleaved H18 segments inside, was recently proposed on the basis of X-ray reflectivity measurements.[8] In the bulk, F*n*H*m* molecules crystallize in a large number of different stable smectic phases, depending on temperature and on *n* and *m* block lengths.[9–11] F*n*H*m* were instrumental in allowing reversible vertical phase separation from phospholipids upon compression of Langmuir monolayers.[12] They allowed substantial stabilization of fluorocarbon-in-water emulsions and control over particle size.[13,14]

F8H16[15] was thoroughly purified by column chromatography, and its purity (> 99 %) determined by GC, TLC, NMR spectroscopy, and elemental analysis. Monolayers were spread from a 1 mM solution of F8H16 in chloroform onto pure water from a milli-Q system. Surface pressure P_s (Wilhelmy plate method) versus molecular area isotherms were recorded at 22.0 ± 0.5 °C on a Langmuir trough (Riegler & Kirstein, Germany) equipped with two movable barriers.

F8H16 formed a monolayer that remained stable up to about 8 mN m^{-1} (Figure 1) with a limiting area of about 30 Å^2 that corresponds to the cross section of a perfluorinated chain, which is larger than that of a typical hydrocarbon chain (ca.

[*] Dr. M. P. Krafft, Dr. M. Maaloum, Dr. P. Muller
Institut Charles Sadron (CNRS)
6, rue Boussingault, 67083 Strasbourg Cedex (France)
Fax: (+ 33) 3-88-41-4099
E-mail: krafft@ics.u-strasbg.fr

[**] This work was supported by the CNRS. We thank AtoFina (Pierre-Bénite, France) for the gift of fluorinated precursors.

  0044-8249/02/11422-4507 $ 20.00+.50/0

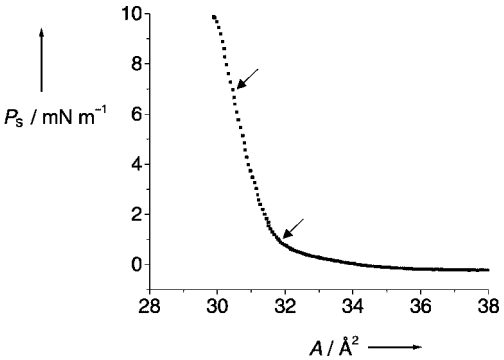

Figure 1. Isotherm of surface pressure P_s versus molecular area A, obtained by compressing F8H16 at an air–water interface at 22 °C. The two arrows indicate the surface pressures of transfer for AFM imaging (Figure 2).

20 Å^2).[16] Because the van der Waals radius of fluorine is larger than half the C–C bond length, steric hindrance causes the chain to adopt a (15/7) helical conformation, which renders the carbon backbone rigid.[17] The isotherm was reversible, without hysteresis, in compression/expansion cycles. The monolayers were transferred onto a silicon wafer, previously treated with a "piranha solution" (conc. H_2SO_4/30 % H_2O_2 3/1) by using the Langmuir–Blodgett technique. The transferred films were analyzed with an atomic force microscope (AFM, NanoScope III) in tapping mode with a nitride cantilever. All scans were performed in the repulsive regime.

Figure 2a shows an AFM image of the F8H16 monolayer transferred at 7 mN m^{-1} onto a silicon wafer. It shows the presence of two-dimensional micelles that form a nanoscale structure on the surface. The AFM images of these surface micelles were analyzed quantitatively by two-dimensional Fourier analysis (Figure 2b). Diffusion rings were observed that originate from hard-core repulsions. For both pressures (0.5 and 7 mN m^{-1}) investigated, the surface micelles have a characteristic diameter of 300 Å. The size distribution of the micelles was highly monodisperse. The average height H of a micelle was assessed by a series of AFM line scans to be 23 ± 5 Å. At 7 mN m^{-1}, the surface micelles pack in an hexagonal arrangement, as assessed by the position of the Bragg peaks (see the two rings in Figure 2b).

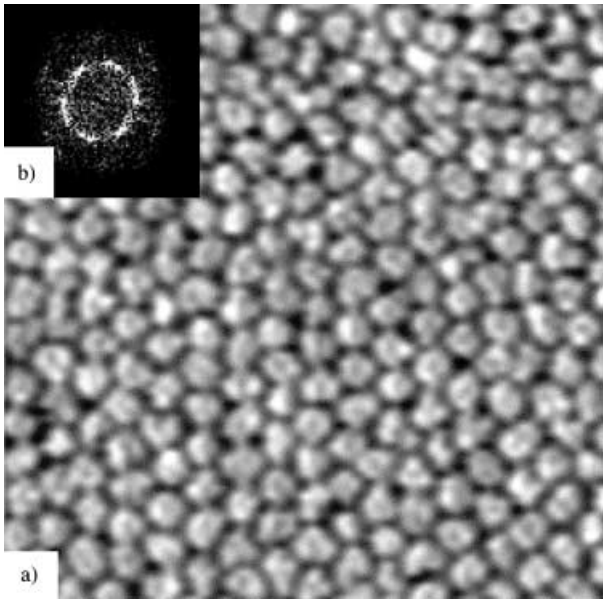

Figure 2. a) AFM image (0.5 × 0.5 μm) of surface micelles in a F8H16 monolayer transferred to a silicon wafer at 7 mN m^{-1}. b) Two-dimensional Fourier transform of (a), showing two rings.

When surface pressure was increased from 0 to 7 mN m^{-1}, the density of the micelles increased progressively. However, the size of the micelles was independent of surface density. When the pressure was further increased to 9 mN m^{-1}, the micelle arrangement became even more compact, but no coalescence between domains was observed.

The F8H16 monolayers were also analyzed by X-ray specular reflectivity. Figure 3 shows X-ray data obtained from a monolayer compressed and transferred at 7 mN m^{-1}. The

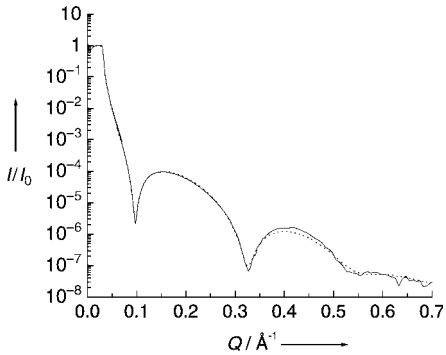

Figure 3. Experimental curve of X-ray reflectivity obtained from the monolayer of F8H16 transferred to a silicon wafer at 7 mN m^{-1}. The dotted curve is the fit obtained with the model in Figure 4a.

experimental curve was fitted to single- and two-layer models with Parratt 32 software. The single-layer model gave poor results, because the corresponding fit always had its second minimum at three times the first minimum, which is clearly not the case in the experimental curve. A two-layer model provided good agreement with the experimental data.

The electron density distribution of the two-layer model (fitted curve in Figure 3) is given in Figure 4a. It consists of an upper layer (in contact with air) with a thickness of 10.0 Å and an electron density of 487 e nm^{-3}, and a lower layer with a thickness of 19.3 Å and an electron density of 290 e nm^{-3}. The total thickness is 29.3 Å. It is noteworthy that the height of the micelle, as measured by X-ray reflectivity, is in close agreement with the length l_C of a fully extended F8H16 molecule, as calculated[18,19] from $l_C = 1.3n + 1.265m + 2.58 = 33.2$ Å for $n = 8$ and $m = 16$). Integration over the whole layer gives a total electron density of $D = 1050$ e nm^{-2}. F8H16 consists of an F8 segment bearing 201 electrons and an H16 segment with 129 electrons. The mean area per molecule is obtained by dividing the total number of electrons of a molecule by D, which gives a molecular area of 31.5 Å^2, which is the value expected if the density is preserved during transfer onto the wafer. However, note that the proportion of electrons in the upper layer is only 46 %, while a simple model in which the fluorinated segments of all molecules point towards air would give an upper layer representing 61 % of the total. Likewise,

  0044-8249/02/11422-4508 $ 20.00+.50/0 *Angew. Chem.* **2002**, *114*, Nr. 22

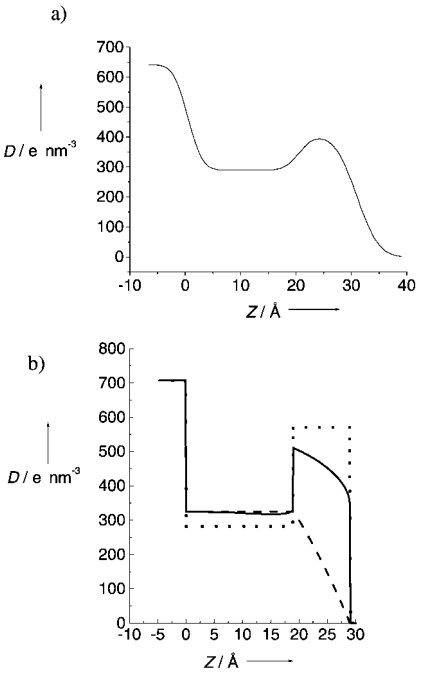

Figure 4. a) Variation of the electron density D as a function of height Z corresponding to the fit of the experimental reflectivity curve (Figure 3). This clearly shows that the first layer is less dense than the second. b) Theoretical electron density profiles (D) for the disklike model (full line) and ellipsoidal model (dashed line) depicted in Figure 5. The density of a homogeneous layer is represented by a dotted line.

the density of the lower layer is larger than that expected for a alkane hydrocarbon layer.

Given the AFM and X-ray data, we tested two models for the shape of the micelles. As the domains are roughly circular, we assumed a circular shape. The X-ray data suggest that the micelle height is close to the length of an extended molecule, but a homogeneous layer of extended molecules whose fluorinated parts point towards air would lead to an unrealistically low density for the hydrocarbon part. Bending the molecules towards the surface at the edge of the domain can substantially reduce this mismatch. The two models that we considered are a disklike shape with quarter circles at the borders and an ellipsoidal shape (Figure 5).

The fluorinated external layer is considered to be composed of rigid F8 rods with a thickness of 11.5 Å and and an area per chain of 30 Å^2. The density of the hydrocarbon part can then be deduced from the molecular constraint by simply calculating the volumes of the two layers. If we set the thickness of the hydrocarbon layer to the measured X-ray value, the mean electron density of the internal hydrocarbon layer becomes a function of the radius R of the micelle. An estimation of the density of the hydrocarbon part can be obtained by using the van der Waals volumes of CH_3 and CH_2 [Eq. (1)] which leads to an electron density of 282 e nm^{-3}. For the disklike model we find $R = 13.0$ nm, while the ellipsoid model gives $R = 15.5$ nm. Varying the density by $\pm 5\,\%$ leads to variation of R from 11.5 to 14.8 nm and from 13.5 to 17.8 nm, respectively. This shows that closing of the domains to reduce the density mismatch provides a reasonable explanation for the observed micelle size.

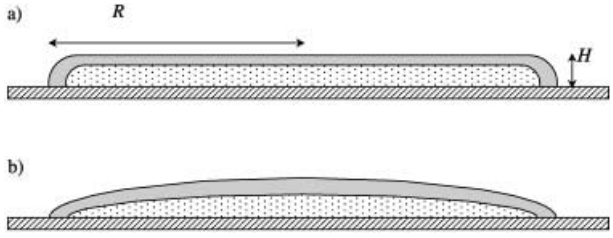

Figure 5. Schematic representation of the cross section of a surface micelle of F8H16 after transfer of the monolayer onto a silicon wafer: a) disklike model; b) ellipsoidal model. The gray area represents the region of fluorinated segments F8, and the dotted area the region of hydrocarbon segments H16.

$$V = V_{CH_3} + 15\,V_{CH_2} = 54.3 + 15 \times 26.9 = 457.8\,\text{Å}^3 \quad (1)$$

We then calculated the theoretical electron density profiles for the two models (Figure 4b). Only the disklike model shows an upper region of higher electron density. Moreover, we can also understand the apparent electron deficiency of the upper layer by comparing the density profile of the disklike model to that of a homogeneous layer. The hydrocarbon volume fraction ϕ_H of the disklike surface micelle can be calculated by using Equation (2) where V_H is the hydrocarbon volume of the surface micelle, $V_F + V_H$ is the total volume, H_H and H_F are the lengths of the fluorinated and hydrocarbon segments of the semifluorinated alkane molecule, and R is the radius of the surface micelle.

$$\phi_H = \frac{V_H}{V_H + V_F} = \frac{\left((R-(H_F+H_H))^2 H_h + \frac{\pi}{2}(R-(H_F+H_H))H_H^2 + \frac{2}{3}H_H^3\right)}{\left((R-(H_F+H_H))^2(H_F+H_H) + \frac{\pi}{2}(R-(H_F+H_H))(H_F+H_H)^2 + \frac{2}{3}(H_F+H_H)^3\right)} \quad (2)$$

Since ϕ_H must be equal to the hydrocarbon volume fraction of the semifluorinated alkane molecule and V_H, V_F, H_H, and H_F depend on m and n, it appears that R is a simple function of n and m. This means that we can predict the size of the surface micelles for a given semifluorinated alkane molecule.

In conclusion, we have found that the nonpolar semifluorinated alkane F8H16 self-assembles into Langmuir monolayers which, transferred to silicon wafers, consist of highly monodisperse stable surface micelles. The hydrocarbon segments of the F8H16 molecules are directed toward the substrate, while the fluorinated segments point outwards toward the air. We demonstrated that the size of these micelles is controlled by the density mismatch between the fluorinated and hydrogenated segments. The radius of the surface micelle is a function of the lengths of the hydrocarbon and fluorinated segments of the FnHm molecules. These results demonstrate the possibility of decorating surfaces with molecular clusters of predetermined size in the nanometer range.

Received: June 21, 2002 [Z19585]

[1] G. G. Warr, *Curr. Opin. Colloid Interface Sci.* **2000**, *5*, 80–94.
[2] J. Zhu, A. Eisenberg, R. B. Lennox, *J. Am. Chem. Soc.* **1991**, *113*, 5583–5588.

  0044-8249/02/11422-4509 $ 20.00+.50/0

[3] O. Albrecht, H. Gruler, E. Sackmann, *J. Phys. (Paris)* **1978**, *39*, 301 – 313.
[4] M. Flörsheimer, H. Möhwald, *Colloids Surf.* **1991**, *55*, 173 – 189.
[5] T. Kato, M. Kameyama, M. Ehara, K. Iimura, *Langmuir* **1998**, *14*, 1786 – 1786.
[6] G. L. Gaines, Jr., *Langmuir* **1991**, *7*, 3054 – 3056.
[7] Z. Huang, A. A. Acero, N. Lei, S. A. Rice, Z. Zhang, M. L. Schlossmann, *J. Chem. Soc. Faraday Trans.* **1996**, *92*, 545 – 552.
[8] A. El Abed, E. Pouzet, M.-C. Fauré, M. Sanière, O. Abillon, *Phys. Rev. E* **2000**, *62*, R5895 – R5898.
[9] J. F. Rabolt, T. P Russell, R. Twieg, *Macromolecules* **1984**, *17*, 2786 – 2794.
[10] T. P. Russell, J. F. Rabolt, R. Twieg, R. L. Siemens, B. L. Farmer, *Macromolecules* **1986**, *19*, 1135 – 1143.
[11] P. Marczuk, P. Lang, M. Möller, *Colloids Surf. A* **2000**, *163*, 103 – 113.
[12] M. P. Krafft, F. Giulieri, P. Fontaine, M. Goldmann, *Langmuir* **2001**, *17*, 6577 – 6584.
[13] J. G. Riess, *Chem. Rev.* **2001**, *101*, 2797 – 2919.
[14] J. G. Riess, *Tetrahedron* **2002**, *58*, 4113 – 4131.
[15] N. O. Brace, *J. Org. Chem.* **1973**, *38*, 3167 – 3172.
[16] A. A. Acero, M. Li, B. Lin, S. A. Rice, M. Goldmann, I. Z. Azouz, A. Goudot, F. Rondelez, *J. Chem. Phys.* **1993**, *99*, 7214 – 7220.
[17] C. W. Bunn, E. R. Howell, *Nature* **1954**, 174, 549 – 541.
[18] C. Tanford, *The Hydrophobic Effect: Formation of Micelles and Biological Membranes*, Wiley, New York, **1973**.
[19] P. Lo Nostro, S. H. Chen, *J. Phys. Chem.* **1993**, *97*, 6535 – 6540.

Novel pH-Reporter MRI Contrast Agents**

Silvio Aime,* Daniela Delli Castelli, and Enzo Terreno

The contrast obtained in magnetic resonance imaging (MRI) relies essentially on differences in the intensity of the ^{1}H water signal. Therefore, the contrast can be augmented by the use of chemicals (contrast agents, CAs) able to enhance the relaxation properties of water protons.[1] Recently, a novel class of paramagnetic CAs has been proposed for MRI applications.[2,3] Such chemicals contain paramagnetically shifted mobile protons whose exchange with the bulk water is slow on the NMR timescale ($|k_{ex}| < |\Delta\omega|$). Thus, irradiation of the mobile protons of the agent determines a decrease of the ^{1}H water signal through the so-called chemical exchange saturation transfer (CEST) effect.[4,5]

One of the major advantages of the CEST agents relies on the possibility of designing responsive agents in which the effectiveness of the CA is not dependent on its concentration. This goal can be pursued when the CEST properties of two independent exchanging pools are monitored in the same experiment (ratiometric method).[6] This possibility has been demonstrated using a mixture of two compounds.[3] An improvement in such ratiometric methods would be obtained if the two proton-exchanging pools were parts of the same molecule (single-molecule CEST procedure). Paramagnetic [Ln(dotamGly)]$^-$ complexes (dotam = 1,4,7,10-tetrakis(carbamoylmethyl)-1,4,7,10-tetrazacyclododecane) would be appropriate for this purpose since they are characterized by the presence of two kinds of mobile protons, namely, the four equivalent amide protons and the two protons of the water molecule coordinated to the Ln^{III} ion. It has been previously shown that the use of a cocktail formed by [Yb(dotamGly)]$^-$ and [Eu(dotamGly)]$^-$ allows the set-up of a ratiometric method for pH measurements by making use of the two exchanging pools provided by the amide protons of the Yb derivative and by the metal-coordinated water protons of the Eu complex, respectively. Herein we demonstrate that the paramagnetic dotamGly complexes of the lighter Ln^{III} ions (Pr, Nd, and Eu) behave as pH-responsive "single-molecule CEST" agents. The efficiency of saturation transfer (ST), once the irradiation time is sufficiently long to reach a steady-state ST value,[3] is directly related to the exchange rate of the irradiated protons (k_{ex}), their molar concentration (defined by the product $n[C]$, where n is the number of irradiated protons and $[C]$ is the molar concentration of the agent), and inversely related to the longitudinal relaxation rate of the bulk water protons during the irradiation $R_{1,irr}$ [Eq. (1)].

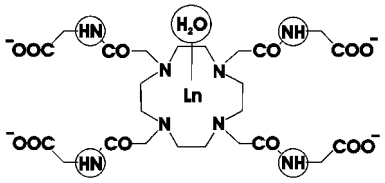

$$ST\,\% = \left(1-\frac{I_S}{I_0}\right)100 = \frac{k_{ex}\,n[C]}{111.2\,R_{1,irr} + k_{ex}\,n[C]}\,100 \qquad (1)$$

The latter parameter, in the presence of a paramagnetic Ln^{III} complex, is mainly determined by the relaxation rate of the metal-coordinated water protons, and this is directly dependent on the intrinsic paramagnetism of the metal ion (μ_{eff}).[7]

I_S and I_0 refer to the intensity of the bulk water signal when the irradiation pulse is set on-resonance (frequency ν^{on}, signal intensity I_S) and off-resonance with respect to the frequency of the bulk water protons ($\nu^{off} = -\nu^{on}$, I_0). The off-resonance measurement is necessary to take into account the direct saturation effect on the bulk water signal which is determined by the irradiation pulse.

The data reported in Figure 1 clearly show that all the three complexes ($[C] = 30$ mM) yield significant ST effects (at 312 K and pH 7.4) upon selective irradiation of their pools of mobile protons. In the case of [Eu(dotamGly)]$^-$, the ST effect from the coordinated water is so efficient that a 10% effect is still detectable when the concentration of the complex is as low as 1 mM. This result makes this system the most efficient CEST agent so far reported if the ST effect is normalized to the number of irradiated spins.[2,4,8] The ST effect from the amide protons $(ST)_{NH}$ follows a reverse order with respect to the

[*] Prof. S. Aime, Dr. D. Delli Castelli, Dr. E. Terreno
Dipartimento di Chimica I.F.M.
Via P. Giuria 7, 10125 Torino (Italy)
Fax: (+39) 011-670-7855
E-mail: silvio.aime@unito.it

[**] Financial support from Bracco Imaging S.p.A., MIUR (PRIN), and CNR (PF Oncology, L. 95/95) are gratefully acknowledged. This work has been carried out under the framework of the EU-COST D 18 action.

  0044-8249/02/11422-4510 $ 20.00+.50/0